Chinese Chemical Letters 34 (2023) 107876

Contents lists available at ScienceDirect

Chinese Chemical Letters

journal homepage: www.elsevier.com/locate/cclet

# Heterogeneous catalytic ozonation by amorphous boron for degradation of atrazine in water

Zirong Song[a], Jie Li[a], Hongxin Xu[b], Yu Li[a], Yaxiong Zeng[c,*], Baohong Guan[a,*]

[a] College of Environmental and Resource Sciences, Zhejiang University, Hangzhou 320058, China
[b] Yiwu Water Construction Group Co., Ltd., Yiwu 322000, China
[c] College of Chemical and Biological Engineering, Zhejiang University, Hangzhou 320013, China

ARTICLE INFO

*Article history:*
Received 4 July 2022
Revised 15 September 2022
Accepted 30 September 2022
Available online 4 October 2022

*Keywords:*
Amorphous boron
Catalytic ozonation
Reactive oxygen species
Atrazine
Advanced oxidation processes

ABSTRACT

As one of the most promising and practical advanced oxidation processes (AOPs), the catalytic ozonation is triggered by the active components of catalyst, which are usually derived from metals or metal oxides. To avoid the metal pollution from catalyst, here the amorphous boron (A-boron) is used as a metal-free catalyst for catalytic ozonation to produce free radicals for effective degradation of atrazine (ATZ), the world-widely used herbicide and also a widespread pollutant in environment. A-boron exhibits an outstanding performance for catalytic ozonation to remove ATZ from water. As A-boron is introduced into ozonation, the degradation efficiency in 10 min is promoted to 97.1%, much higher than that of 15.1% under ozonation. The mechanism is that the B–B bonds and internal suboxide B in A-boron serve as the main active sites to donate electrons to accelerate ozone decomposition to produce reactive oxygen species (ROS), including $^{\bullet}O_2^-$ and $^1O_2$, and further enhance ATZ degradation *via* ROS reactions. Moreover, the A-boron is still highly active with a degradation efficiency of ATZ over 95% in 10 min even after four successive cycles. This work shows A-boron could be an alternative for the active components of metal or metal oxide in catalytic ozonation.



Atrazine (ATZ), a kind of organochlorotriazine herbicide [1], is used to control a variety of annual herbs and broad-leaved weeds due to its extensive insecticidal spectrum [2]. However, ATZ is suspected to be an endocrine disruptor to cause genotoxicity, mutagenicity, and hormonal imbalance [3,4]. As one of the persistent organic pollutants (POPs), ATZ migrates easily in the environment [1,5], and has even been found in groundwater in many countries [6,7]. The traditional methods such as coagulation, flocculation, filtration and chlorination in municipal wastewater treatment plant cannot remove ATZ efficiently [8–11], while advanced oxidation processes (AOPs) can rapidly degrade and mineralize it through radical reactions, which is triggered by exciting chlorides, hydrogen peroxide, persulfate, ozone and other oxidants to produce free radicals with high redox potential [12–15]. Among these AOPs, the way based on ozonation is an attractive option for removing ATZ from water thanks to the high oxidation potential (2.07 V *vs.* NHE) and no secondary pollution. The ozonation to degrade organic pollutants follows two ways: (1) Direct electrophilic attack of ozone molecules; (2) indirect attack by radicals generated by ozone decomposition and chain reactions [16]. Obviously, the latter has the advantage to produce reactive oxygen species (ROS), including $^{\bullet}OH$, $^{\bullet}O_2^-$, $^1O_2$, so as to achieve high reaction rate for ATZ degradation. For example, the reaction rate constant of ozonation for ATZ ($k(O_3/ATZ)$) is 6 L mol$^{-1}$ s$^{-1}$, while the one of catalytic ozonation with hydroxyl radicals for ATZ ($k(^{\bullet}OH/ATZ)$) tremendously reaches $3 \times 10^9$ L mol$^{-1}$ s$^{-1}$ [17]. Hence the catalytic ozonation with extraordinary ROS reaction attracts heavy attentions for the treatment of water or wastewater containing pesticides and herbicides.

The catalytic ozonation, which works with the free radicals triggered by metal-based catalysts, such as $FeO_x$ [18–20], $MnO_x$ [20,21] and MgO [22], has been widely used to improve the degradation of organic pollutants. Unfortunately, the active component in metal-based catalysts is easy to fall off, leading to the leaching of toxic metal [23]. The metal-free carbon-based catalysts have attracted attention in catalytic ozonation for their good electron transfer ability and no metal ion leaching [23,24]. However, the activity of the metal-free carbon-based catalysts decreases seriously after reuse [25–27]. Thus, a kind of metal-free catalyst with stable performance for catalytic ozonation to obtain high activity in the degradation of organic pollutants is in urgent need in water and wastewater treatment. Boron, which is very similar to carbon

* Corresponding authors.
*E-mail addresses:* zengyaxiong@zju.edu.cn (Y. Zeng), guanbaohong@zju.edu.cn (B. Guan).

https://doi.org/10.1016/j.cclet.2022.107876
1001-8417/

on the scale of atomic clusters [28], is a strong electron donor [29], and thus has the potential as a catalyst in catalytic ozonation. Zhou *et al.* employed crystalline boron to accelerate $Fe^{III}/Fe^{II}$ circulation in Fenton-like systems (C-Boron/$Fe^{III}/H_2O_2$) to produce a myriad of hydroxyl radicals [30]. Shao *et al.* have discovered that the amorphous boron has better catalytic performance than crystalline boron, and attributed it to the long-range disorder atom arrangement and the pretty localized electron states of amorphous boron, which are beneficial for the electrons transfer than crystalline boron [29,31]. Moreover, ozone is electrophilic, and tends to be decomposed into ROS after accepting electrons, so as to improve the removal efficiency of organic pollutants [32–34]. However, there are few studies on the application of boron in catalytic ozonation for water treatment.

Here we employ amorphous boron (A-boron) in catalytic ozonation to produce free radicals with high redox potential for degrading ATZ in water. The active sites and the mechanisms for catalytic ozonation by A-boron are elucidated, and the stability of A-boron is also investigated. With the evaluation on performances and mechanisms of ATZ degradation in regard to the $O_3$/A-boron, we develop a metal-free catalyst for catalytic ozonation. Finally, the potential characteristics and advantages of A-boron have been summarized.

Figs. 1a and b show the disordered lattice fringes and the homogenous diffraction pattern of diffused intensity rings, indicating the disorder atom arrangement of A-boron. Also, the diffraction peak of A-boron does not match the standard PDF table of boron (PDF #06–0297) detected by XRD (Fig. S1 in Supporting information) and the irregular shapes of A-boron nanoparticles detected by SEM (Fig. S2 in Supporting information) demonstrate the amorphous properties of A-boron. Fig. 1c shows the B 1s XPS spectrum of the A-boron. The peak centered at 187.02 eV is attributed to the B–B bond [35]. The peak centered at 188.48 eV corresponds to the internal suboxide B [29,35], which is the partially oxidized Boron of the B–B bond. The binding energy of $B_2O_3$ in A-boron shows a red shift from the standard binding energy of 193.1 eV [36] to 191.43 eV, which is attributed to the electron supply capacity of B–B bonds and internal suboxide B [37], and thus enhances the

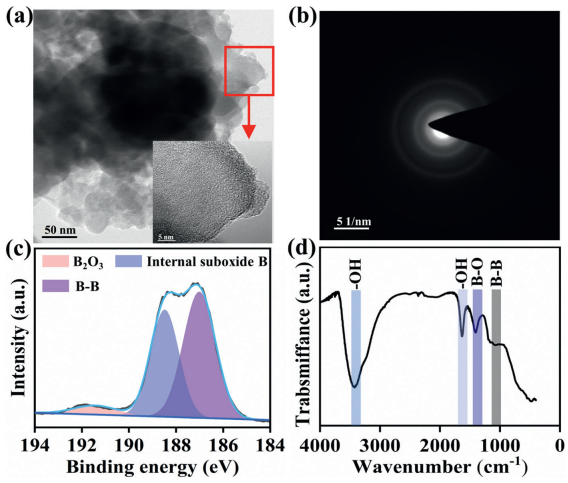


**Fig. 1.** TEM images (a), SAED pattern (b), B 1 s XPS (c), FTIR spectrum (d) of A-boron.

electron cloud density around $B_2O_3$. Moreover, the bonding characteristics of the B–B bond in A-boron is also detected in FT-IR spectrometer (Fig. 1d), which is in good agreement with the analysis of XPS. The vibration band around 1200 $cm^{-1}$ represents the B–B bond of A-boron [29]. The absorption peaks at 1406 $cm^{-1}$ is due to the asymmetric stretching vibration of trigonal B–O bonds in $B_2O_3$ [38,39]. The peaks near 1629 $cm^{-1}$ and 3424 $cm^{-1}$ are attributed to the −OH vibration and stretching, which are usually caused by the adsorption of $H_2O$ [40]. The −OH group is often regarded as an important active site for catalytic ozonation [16]. In addition, the B–B bonds and the internal suboxide B are beneficial for facilitating the electrons transfer [37]. Therefore, the role of B–B bonds, internal suboxide B and −OH group in catalytic ozonation will be explored later.

Fig. 2a shows the removal efficiencies of ATZ by ozonation ($O_3$), A-boron adsorption, and A-boron catalytic ozonation

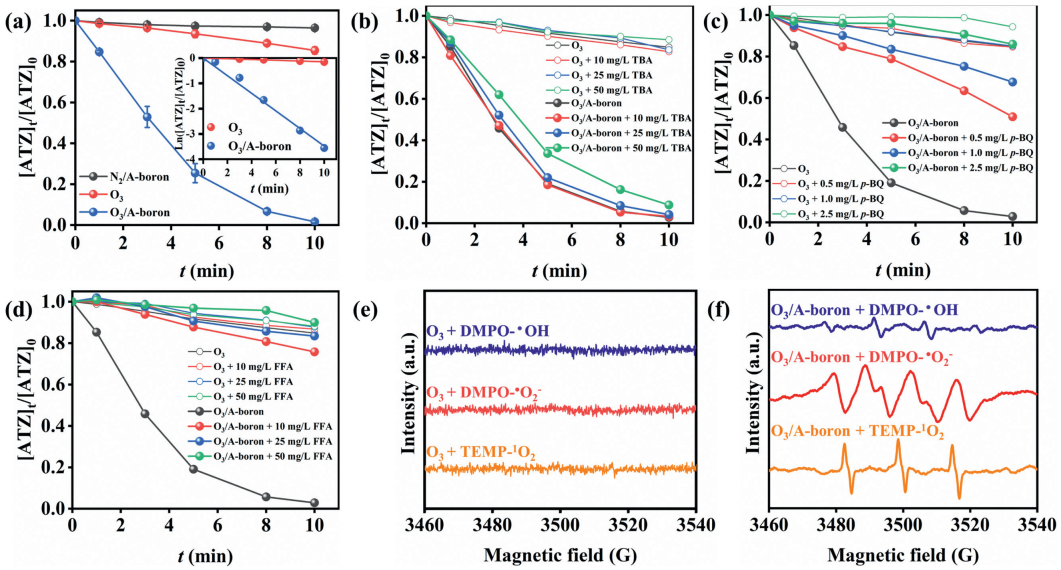


**Fig. 2.** The removal of ATZ by ozonation, A-boron adsorption and $O_3$/A-boron (a). Influences of radical scavengers including *tert*–butyl alcohol (TBA, 10, 25, 50 mg/L) (b), *p*-benzoquinone (*p*-BQ, 0.5, 1.0 and 2.5 mg/L) (c), and furfuryl alcohol (FFA, 10, 25 and 50 mg/L) (d) on ATZ degradation. EPR spectra of $O_3$ (e) and $O_3$/A-boron (f). Conditions: $T = 20$ °C, $[ATZ]_0 = 1.0$ mg/L, $[A\text{-boron}]_0 = 25.0$ mg/L, $[O_3]_{input} = 2.0$ mg/L, initial pH 6.99, gas flow rate of 0.4 L/min. EPR spectra for the detection of •OH in the presence of 5,5-dimethyl-1-pyrrolidine-*N*-oxide (DMPO, 100 mmol/L), using water as the solvent. EPR spectra for the detection of $^{\bullet}O_2^-$ in the presence DMPO (100 mmol/L), using methanol as the solvent. EPR operating conditions using DMPO: Centerfield, 3502.0 G; sweep width, 100.0 G; microwave frequency, 9.825 GHz; modulation frequency, 100.0 kHz; power, 6.325 mW. EPR spectra for the detection of $^1O_2$ in the presence of 2,2,6,6-tetramethylpiperidine (TEMP, 100 mmol/L), using water as the solvent. EPR operating conditions using TEMP: centerfield, 3502.00 G; sweep width, 100.0 G; microwave frequency, 9.827 GHz; modulation frequency, 100 GHz; power, 6.325 mW.

($O_3$/A-boron) in 10 min. The adsorption of ATZ by A-boron with nitrogen gas bubbling ($N_2$/A-boron) is responsible for less than 2.5% ATZ removal, which is deducted as a background value of ozonation or $O_3$/A-boron. The ozonation removes 15.1% ATZ, while $O_3$/A-boron achieves 97.1% removal efficiency, proving that the catalytic ozonation by A-boron obtains much higher removal efficiency than ozonation. The degradation processes of ATZ by ozonation and $O_3$/A-boron are well-fitted by pseudo-first-order kinetic model (Fig. 2a, inset). The ATZ degradation rate constant ($k_{obs}$) of 0.360 $min^{-1}$ obtained in $O_3$/A-boron is 24 times that of 0.015 $min^{-1}$ in ozonation, suggesting that the A-boron plays a key role in the catalytic ozonation of ATZ.

Fig. S3 (Supporting information) illustrates the catalytic ozonation activity of A-boron and several commonly used metal-free carbon-based catalysts for ATZ degradation under the same reaction conditions. The removal efficiencies of ATZ by catalytic ozonation with carbon nanotube (CNT), graphene oxide (GO) and graphitic carbon nitride (g-$C_3N_4$) in 10 mins are 81.7%, 36.7% and 25.7%, respectively, which are much lower than that of A-boron (97.1%), indicating A-boron has higher catalytic ozonation performance than CNT, GO and g-$C_3N_4$.

Furthermore, the intrinsic activity of the catalyst can be represented by the turnover frequency (TOF), which is calculated by dividing $k_{obs}$ by the amount of catalyst [41,42]. The higher the TOF value indicates the better catalytic ozonation performance for ATZ degradation, and thus the higher activity of the catalyst. Evidently, A-boron with the highest TOF value and the lowest ozone dosage exhibits the best catalytic performance among all catalysts shown in Table S1 and Fig. S4 (Supporting information). Also, TOC changes are measured to further evaluate the mineralization efficiency of $O_3$ and $O_3$/A-boron. Fig. S5 (Supporting information) shows the ozonation removes 11.0% of TOC, which $O_3$/A-boron removes 36.6% of TOC, proving that the catalytic ozonation by A-boron obtains much higher TOC removal efficiency than ozonation.

The removal efficiency of organic pollutants is largely dependent on the initial pH of the solution [16]. Hence, the effect of initial pH (from 3.69 to 10.98) on ATZ removal by $O_3$/A-boron was investigated. The removal efficiencies of ATZ by $O_3$/A-boron increase from 82.6% to 87.2%, 96.3%, 97.1% and 97.5% with increasing initial pH from 3.69 to 5.12, 6.99, 8.97 and 9.96, then no significant change occurs with further increasing initial pH to 9.96 and 10.98 (Fig. S6 in Supporting information), indicating that increasing the initial pH improves the degradation efficiency of ATZ by $O_3$/A-boron, and A-boron exhibit high efficiency over a wide range of pH values. The wide pH application ranges of A-boron are related to the points of zero charge ($pH_{pzc}$) of A-boron. Fig. S7 (Supporting information) shows the $pH_{pzc}$ of A-boron is about 3.6. When $pH > pH_{pzc}$, the negative charges occur on the surface of A-boron, and thus the intensity increases with the increase of pH, such as $\Delta$pH is −0.49, −2.09, −3.24 and −3.88, corresponding to the pH of 5.65, 6.99, 8.75 and 10.97, respectively. Ozone molecules prefer to adsorb on the surface of A-boron with negative charges rather than with positive charges due to its electrophilicity [43]. Therefore, a higher pH value is helpful for ozone molecules adsorption and ROS production.

ROS of hydroxyl radicals ($^{\bullet}OH$), superoxide radicals ($^{\bullet}O_2^-$) and singlet oxygen ($^1O_2$) are commonly considered as the potential radical species in the process of catalytic ozonation [33]. To identify the primary ROS for the degradation of ATZ, the quenching tests were carried out by using *tert*–butyl alcohol (TBA), *p*-benzoquinone (*p*-BQ), and furfuryl alcohol (FFA) as scavengers of $^{\bullet}OH$, $^{\bullet}O_2^-$, $^1O_2$, respectively[23].

Fig. 2b shows that 10, 25 and 50 mg/L of TBA have a little effect on the degradation of ATZ by ozonation and $O_3$/A-boron with less than 10% decrease in removal efficiencies, indicating that $^{\bullet}OH$ has little contribution to the ATZ degradation. Fig. 2c depicts the effect of *p*-BQ with various dosages (0.5, 1.0 and 2.5 mg/L) on the ATZ removal efficiency by ozonation and $O_3$/A-boron, and the results show that 0.5 mg/L and 1.0 mg/L *p*-BQ have a slight effect on the ozonation to degrade ATZ, but a significant effect on the catalytic ozonation by $O_3$/A-boron to degrade ATZ. When *p*-BQ dosages are increased from 0 to 0.5 mg/L and 1.0 mg/L, the removal efficiencies are correspondingly reduced from 97.1% to 49.1% and 32.3%, indicating that $^{\bullet}O_2^-$ is the main ROS and plays a dominant role in the catalytic ozonation by $O_3$/A-boron. FFA acts as a scavenger not only for $^1O_2$ ($k(FFA/^1O_2) = 1 \times 10^8$ L $mol^{-1}$ $s^{-1}$), but also for $^{\bullet}OH$ ($k(FFA/^{\bullet}OH) = 1.5 \times 10^{10}$ L $mol^{-1}$ $s^{-1}$) [33,44,45]. After ruling out the existence of ·OH, FFA was used to detect whether there is $^1O_2$ in the process of ATZ degradation by $O_3$/A-boron. Fig. 2d shows that 10, 25 and 50 mg/L FFA have a slight effect on the ozonation to degrade ATZ, but a prominent effect on the catalytic ozonation by $O_3$/A-boron to degrade ATZ. When FFA dosages are raised from 0 to 10, 25 and 50 mg/L, the removal efficiencies are accordingly cut down from 97.1% to 25.1%, 16.6% and 10.0%, implying that $^1O_2$ is the main ROS in the catalytic ozonation by $O_3$/A-boron.

To accurately illustrate the ROS species in ozonation and catalytic ozonation, EPR tests were performed to capture ROS for ATZ degradation, and DMPO and TEMP are typical trapping chemicals for $^{\bullet}OH$/$^{\bullet}O_2^-$ and $^1O_2$ [23]. However there are no detectable $^{\bullet}OH$/$^{\bullet}O_2^-$ and $^1O_2$ signals in ozonation (Fig. 2e), indicating that neither $^{\bullet}OH$/$^{\bullet}O_2^-$ nor $^1O_2$ is responsible for the degradation of ATZ in ozonation. By contrast, the quadruple peak signal with the ratio of 1:2:2:1, 1:1:1:1 and the triple peak signal with the ratio of 1:1:1, which are assigned to DMPO-$^{\bullet}OH$, DMPO-$^{\bullet}O_2^-$ and TEMP-$^1O_2$ adduct characteristic peaks, respectively, are clearly observed in $O_3$/A-boron (Fig. 2f). Especially, the intensities of DMPO-$^{\bullet}O_2^-$ and TEMP-$^1O_2$ signals are obviously stronger than that of DMPO-$^{\bullet}OH$, implying that more $^{\bullet}O_2^-$ and $^1O_2$ are formed in catalytic ozonation. Both the quenching test and the EPR test show that $^{\bullet}O_2^-$ and $^1O_2$ are the dominant ROS, which are responsible for the degradation of ATZ in $O_3$/A-boron.

The XPS of B 1s region of the fresh A-boron and the fifth time used A-boron shown in Fig. 3a explains that the relative content of the B–B bonds in A-boron decreases from 54.6% to 51.7% after five times use in catalytic ozonation, while that of internal suboxide B increases from 40.9% to 43.3%, and that of $B_2O_3$ increases from 4.5% to 5.0%. That is, a small amount of B–B bonds is oxidized and converted into internal suboxide B and $B_2O_3$ in the catalytic ozonation. During the conversion, the B–B bonds in A-boron work as an active component for catalytic ozonation. The effect of the internal suboxide B on catalytic ozonation is revealed by Fig. 3b. Tetrahydroxydiboron (THDB), as a model molecule of the internal suboxide B [37], improves the ATZ degradation efficiency from 15.1% in ozonation to 41.9% in $O_3$/THDB in 10 min, suggesting that the internal suboxide B is also the active site for catalytic ozonation. The B–B bonds together with the internal suboxide B in A-boron act as the active sites to accelerate the electrons transfer and enhance ROS production [37], and thus results in the catalytic ozonation for promoting the degradation of ATZ.

To further explore the effect of $B_2O_3$ on catalytic ozonation for the degradation of ATZ, the XPS spectra and the corresponding relative contents of $B_2O_3$ of A-boron samples after thermal treatment at 300 °C, 500 °C and 700 °C, which are labelled A-boron-300, A-boron-500 and A-boron-700, respectively, are shown in Fig. S8 (Supporting information) and Table 1. The relative contents of $B_2O_3$ in fresh A-boron, A-boron-300, A-boron-500 and A-boron-700 are 4.45%, 14.40%, 61.18%, and 100%, which increase with increasing thermal treatment temperature. The ATZ removal by catalytic ozonation with $B_2O_3$, A-boron or A-boron with different $B_2O_3$ content caused by different thermal treatment temperature are shown in Figs. 3c and d. Obviously, $B_2O_3$ does not present any catalytic effect on the ozonation. In addition, the degradation effi-

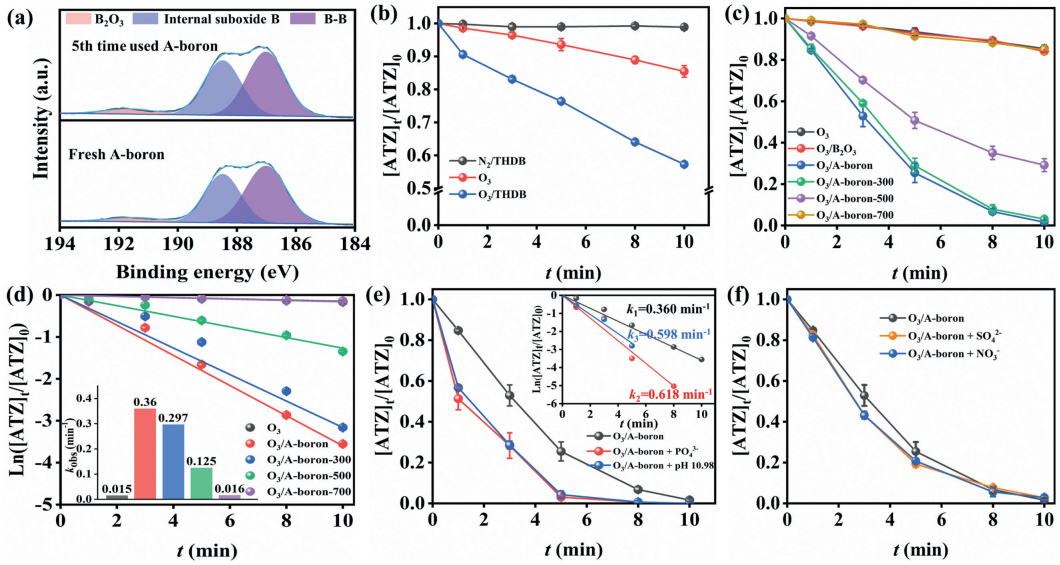


**Fig. 3.** B 1s XPS spectrum of the fresh A-boron and the 5th time used A-boron (a). The degradation efficiencies of ATZ in catalytic ozonation resulted from tetrahydroxydiboron (THDB) (b). The degradation efficiency of ATZ by catalytic ozonation with A-boron calcined at different temperatures to show the catalytic effects of contents of $B_2O_3$ (c). *Pseudo*-first-order kinetics data fitting for catalytic ozonation with A-boron under different calcified temperature to further confirm the catalytic effect (d). Effects of 100 mg/L phosphate (e), 100 mg/L nitrate and 100 mg/L sulfate (f) on degradation efficiency of ATZ by $O_3$/A-boron. Conditions: $T = 20$ °C, $[ATZ]_0 = 1.0$ mg/L, $[A\text{-boron}]_0 = 25.0$ mg/L, $[O_3]_{input} = 2.0$ mg/L, initial pH 6.99, gas flow rate of 0.4 mg/L.

**Table 1**
The relative contents of B–B bonds, internal suboxide B and $B_2O_3$ in fresh A-boron, A-boron-300, A-boron-500.

| Substance | B–B bonds contents | Internal suboxide B contents | $B_2O_3$ contents |
|---|---|---|---|
| Fresh A-boron | 54.63% | 40.92% | 4.45% |
| A-boron-300 | 45.80% | 39.80% | 14.40% |
| A-boron-500 | 21.80% | 17.02% | 61.18% |

ciency of ATZ decreases from 97.1% to 95.7%, 73.9%, and 12.9% in 10 min, with $B_2O_3$ contents increased from 4.45% to 14.40%, 61.18%, and 100%, respectively, indicating that the increase in $B_2O_3$ content in A-boron sample deteriorates the catalytic ozonation, so as to reduce the degradation rate of ATZ. This phenomenon is also validated by the negative relationship between ATZ degradation rate constant $k_{obs}$ and $B_2O_3$ contents in A-boron sample (Fig. S9 in Supporting information). However, the decrease content of B–B bonds and internal suboxide B in A-boron samples results in the ATZ degradation rate constant $k_{obs}$ decrease from 0.360 $min^{-1}$ to 0.016 $min^{-1}$ (Figs. S10 and S11 in Supporting information), suggesting that the B–B bonds and internal suboxide B in A-boron samples play a positive role in catalytic ozonation, which further confirm the B–B bonds and internal suboxide B to be the active sites of catalytic ozonation.

The −OH groups at the acid sites of the catalyst are usually regarded as the active sites [46], which are always demonstrated with the experiment of phosphate scavenging hydroxyl active sites on catalyst surface [47,48]. Fig. 3e shows the trisodium phosphate promotes rather than suppresses the degradation of ATZ with rate constant $k_{obs}$ increases from 0.360 $min^{-1}$ to 0.618 $min^{-1}$ by $O_3$/A-boron, indicating that the −OH groups at the acid sites of A-boron samples are not the active sites for catalytic ozonation. In addition, the ATZ molecules are positively charged as the pH of the solution is higher than its p$K_a$ (1.7), and are then more easily attacked by $^{\bullet}O_2^-$ [49,50]. Meanwhile, $^1O_2$ react preferentially with electron-rich moieties in organic pollutants like ATZ [51–53]. Thus, $^{\bullet}O_2^-$ and $^1O_2$ prefer to attack ATZ rather than react with phosphate. However, the pH of the solution increased to 10.98 after adding 100 mg/L phosphate. Coincidently, at the pH of 10.98, the ATZ removal rate constant $k_{obs}$ by $O_3$/A-boron is 0.598 $min^{-1}$ (Fig. S12 in Supporting information), which is very close to that of 0.618 $min^{-1}$ under the condition of adding 100 mg/L phosphate, indicating that the improved efficiency of ATZ removal after adding phosphate is resulted from the increase of solution pH by the hydrolysis of phosphate. That is, the hydrolysis of phosphate leads to an increase in the pH of solution and thus facilitates the generation of $^{\bullet}OH$ by ozone through chain reaction [23], and further improves the degradation of ATZ by $O_3$/A-boron. Xu *et al.* also found that the addition of phosphate improved the performance of ozonation through increasing solution pH [26]. Sodium nitrate and sodium sulfate are believed to inhibit the activity of the catalyst by replacing the −OH groups on the surface of the catalyst [54,55]. However, neither 100 mg/L sodium sulfate nor 100 mg/L sodium nitrate has distinct effect on the degradation efficiency of ATZ by $O_3$/A-boron (Fig. 3f), supporting that the −OH groups in A-boron does not play a catalytic role in ozonation. Therefore, the B–B bonds and internal suboxide B other than the −OH groups at the acid sites are the active sites for catalytic ozonation.

How can the B–B bonds and internal suboxide B act as active sites to generate ROS? The disordered atomic arrangement of A-boron destroys the geometrical symmetry of $B_{12}$ icosahedron, and causes an asymmetrical distribution of charge density in B–B bonds [29], resulting in a polarization of the B–B bonds and reverse charging [37], and consequently turns the B–B bonds to the negative and positive electrodes. Fig. S7 also shows the A-boron surface is negatively charged at pH 6.99. The negative electrode accepts oxygen atoms to form internal suboxide B ($B^+$-$B^+$-$O^{\bullet}$) and produce $^{\bullet}O_2^-$ according to Eq. 1. Then, the formed $B^+$-$B^+$-$O^{\bullet}$ facilitates $O_3$ decomposition to generate $^{\bullet}O_2^-$ through electron transfer and simultaneously produces $B^{III}$-O, as shown in Eq. 2. Subsequently, $B^{III}$-O is turned to $H_3BO_3$, and $^{\bullet}O_2^-$ tends to transfer to $^1O_2$ rather than $^{\bullet}OH$ in $O_3$/A-boron, according to Eqs. 3 and 4.

$$B^+\text{-}B^- + O_3 \rightarrow B^+\text{-}B^-\text{-}O\text{-}O\text{-}O^- \rightarrow B^+\text{-}B^+\text{-}O^{\bullet} + {}^{\bullet}O_2^- \quad (1)$$

$$B^+\text{-}B^+\text{-}O^{\bullet} + O_3 \rightarrow 2B^{III}\text{-}O^{\bullet} + {}^{\bullet}O_2^- \quad (2)$$

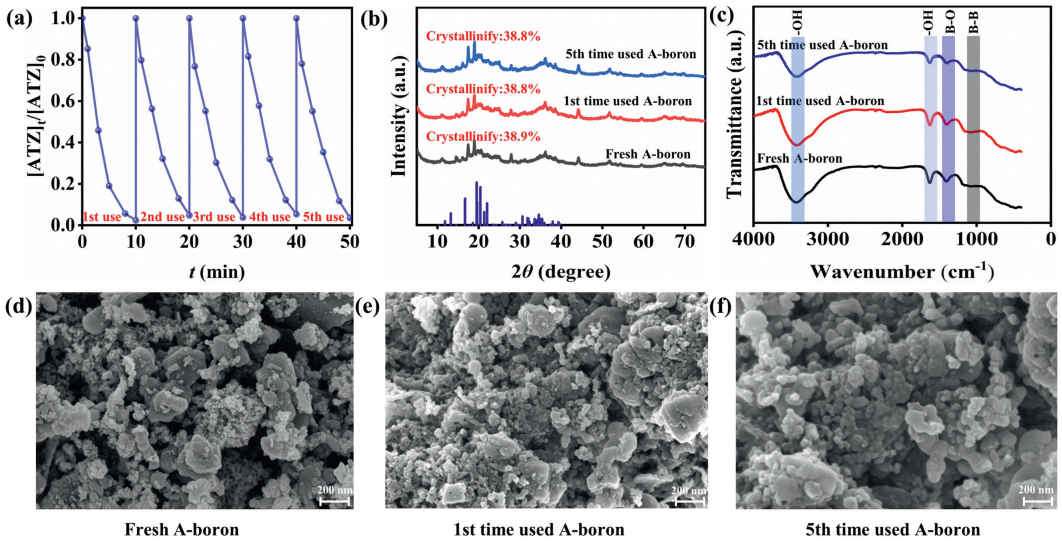


**Fig. 4.** The ATZ degradation efficiency by catalytic ozonation with reused A-boron to show the stability of the catalyst activity (a). XRD (b), FTIR (c) and SEM (d-f) patterns of A-boron. 1st time used A-boron stands for A-boron with one time used and 5th time used A-boron stands for A-boron with five time used. Conditions: $T = 20$ °C, $[ATZ]_0 = 1.0$ mg/L, $[A\text{-boron}]_0 = 25.0$ mg/L, $[O_3]_{input} = 2.0$ mg/L, initial pH 6.99, gas flow rate of 0.4 L/min.

$$3B^{III}\text{-}O^{\bullet} + H_2O \rightarrow 2H_3BO_3 \quad (3)$$

$$^{\bullet}O_2^- + 2H_2O \rightarrow {}^1O_2 + H_2O_2 + 2OH^- \quad (4)$$

Thus, the possible mechanisms of ATZ degradation in the $O_3$/A-boron are that the B–B bonds and internal suboxide B in A-boron serve as the main active sites to donate electrons to ozone molecules and start the chain reaction for the generation of the ROS of $^{\bullet}O_2^-$ and $^1O_2$, which are responsible for the ATZ degradation through ROS reactions.

The stability is an important index to the performance of catalyst for ozonation. As the A-boron dosage was fixed at 25 mg/L in $O_3$/A-boron, the concentration of boron ions leaching from A-boron after 10 min catalytic ozonation were detected to be in a range of 0.301–0.342 mg/L in four successive cycles, which is far below the limited value of 2.4 mg/L in drinking water recommended by the WHO [56]. Fig. 4a depicts the ATZ degradation efficiency by catalytic ozonation with reused A-boron. The reused A-boron still achieves more than 95% efficiency in ATZ degradation in 10 min after four successive cycles. By contrast, the removal efficiencies of ATZ in 10 min by catalytic ozonation with CNT, GO and g-$C_3N_4$ decrease from 81.7%, 36.7% and 25.7% to 53.4%, 28.3% and 18.0%, respectively, after four successive cycles (Fig. S13 in Supporting information), indicating that the carbon-based catalysts present a great decline in the catalytic performance after several times reuse. The similar results have been reported by several researchers. For example, the three reused fluorine-doped CNTs witnesses a remarkable decrease in the degradation efficiency of oxalic acid by catalytic ozonation from 83% to 65% [25], and the five reused graphene finds an activity weakening in the removal efficiencies of cephalexin removal by catalytic ozonation from 50.3% to 32.4% [26].

The XRD patterns in Fig. 4b show the reused A-boron keeps the same crystalline phase and almost the same crystallinity of 38.8%−38.9% with the fresh A-boron. The FT-IR spectra in Fig. 4c confirm that the B–B bonds as the active sites of A-boron remain unchanged after four successive cycles. Figs. 4d-f show that even after the fifth use, the A-boron almost maintains its original morphology and structure with disorder arrangement. So it can be verified that the reused A-boron keeps stable performance and crystalline properties.

A-boron, a metal-free catalyst, exhibits excellent performance and stability in the catalytic ozonation for the removal of ATZ from water. A-boron catalytic ozonation achieves 24 times ATZ degradation rate constant than ozonation. The B–B bonds and internal suboxide B in A-boron act as active sites for molecular ozone decomposition to generate ROS of $^{\bullet}O_2^-$ and $^1O_2$, which predominate in the $O_3$/A-boron. The negative electrodes formed by the polarization of B–B bonds in A-boron accept oxygen atoms and promote the electrons transfer, so improve the ROS reaction activity to degrade organic compounds, holding promise for water remediation. This work could bring extendibility to prepare A-boron based catalysts for catalytic ozonation used for organic pollutants removal from water and wastewater.

## Declaration of competing interest

The authors declare that they have no known competing financial interests or personal relationships that could have appeared to influence the work reported in this paper.

## Acknowledgments

Financial support is provided by the Key Research and Development Program of Zhejiang Province (No. 2021C03179) and the National Key Research and Development Program of China (No. 2019YFC0408802).

## References

[1] A.A. Esquerdo, I.S. Gadea, P.J.V. Galvan, D.P. Rico, Sci. Total Environ. 764 (2021) 144301.
[2] J. Gomes, R. Costa, R.M.Q. Ferreira, R.C. Martins, Sci. Total Environ. 586 (2017) 265–283.
[3] C.B. Breckenridge, P.S. Coder, M.O. Tisdel, et al., Birth. Defects. Res. B 104 (2015) 204–217.
[4] S.A. Abdulelah, K.G. Crile, A. Almouseli, et al., Chemosphere 239 (2020) 124786.
[5] A.N. Kabra, M.K. Ji, J. Choi, et al., Environ. Sci. Pollut. Res. Int. 21 (2014) 12270–12278.
[6] J. Ge, J. Cong, Y. Sun, et al., Bull. Environ. Contam. Toxicol. 84 (2010) 401–405.
[7] A.S. Sousa, W.C. Duavi, R.M. Cavalcante, M.A. Milhome, R.F.D. Nascimento, Bull. Environ. Contam. Toxicol. 96 (2016) 90–95.
[8] S. Singh, V. Kumar, A. Chauhan, et al., Environ. Chem. Lett. 16 (2017) 211–237.
[9] J. Lharidon, M. Fernandez, V. Ferrier, J. Bellan, Water Res. 27 (1993) 855–862.
[10] M.J.M. Bueno, A. Aguera, M.J. Gomez, et al., Anal. Chem. 79 (2007) 9372–9384.
[11] Y. Liu, S. Wang, L. Shi, W. Lu, P. Li, Environ. Sci. Water Res. Technol. 6 (2020) 1681–1687.

[12] X. Kong, J. Jiang, J. Ma, et al., Water Res. 90 (2016) 15–23.
[13] Y. Ji, C. Dong, D. Kong, J. Lu, J. Hazard. Mater. 285 (2015) 491–500.
[14] H. Li, B. Zhou, J. Environ. Sci. Heal. B 54 (2019) 432–440.
[15] J. Li, Y. Li, Z. Xiong, G. Yao, B. Lai, Chin. Chem. Lett. 30 (2019) 2139–2146.
[16] J. Wang, Z. Bai, Chem. Eng. J. 312 (2017) 79–98.
[17] J.L. Acero, K. Stemmler, U.V. Gunten, Environ. Sci. Technol. 34 (2000) 591–597.
[18] R.H. Huang, J. Liu, L.S. Li, et al., Chin. Chem. Lett. 22 (2011) 683–686.
[19] Z. Xiong, B. Lai, Y. Yuan, et al., Chem. Eng. J. 302 (2016) 137–145.
[20] S.Q. Tian, J.Y. Qi, Y.P. Wang, et al., Water Res. 193 (2021) 116860.
[21] X. Tan, Y. Wan, Y. Huang, et al., J. Hazard. Mater. 321 (2017) 162–172.
[22] T. Shen, Q. Wang, S. Tong, Ind. Eng. Chem. Res. 56 (2017) 10965–10971.
[23] Y. Xie, Y. Liu, Y. Yao, et al., Chin. Chem. Lett. 33 (2022) 1298–1302.
[24] J. Restivo, C.A. Orge, A.S.G.G. Santos, O.S.G.P. Soares, M.F.R. Pereira, Catal. Today 384 (2022) 187–196.
[25] J. Wang, S. Chen, X. Quan, H. Yu, Chemosphere 190 (2018) 135–143.
[26] J. Xu, Y. Li, M. Qian, et al., Appl. Catal. B: Environ. 256 (2019) 117797.
[27] A.S.G.G. Santos, C.A. Orge, O.S.G.P. Soares, M.F.R. Pereira, J. Water Process. Eng. 38 (2020) 101573.
[28] A.J. Mannix, X.F. Zhou, B. Kiraly, et al., Science 350 (2015) 1513–1516.
[29] P. Shao, X. Duan, J. Xu, et al., J. Hazard. Mater. 322 (2017) 532–539.
[30] P. Zhou, W. Ren, G. Nie, et al., Angew. Chem. Int. Ed. 59 (2020) 16517–16526.
[31] L. Ge, S. Lei, A.H.C. Hart, et al., Nanotechnology 25 (2014) 335701.
[32] U.V. Gunten, Water Res. 37 (2003) 1443–1467.
[33] G. Yu, Y. Wang, H. Cao, H. Zhao, Y. Xie, Environ. Sci. Technol. 54 (2020) 5931–5946.
[34] X. Luo, T. Su, X. Xie, Z. Qin, H. Ji, ChemistrySelect 5 (2020) 15092–15116.
[35] B. Feng, J. Zhang, Q. Zhong, et al., Nat. Chem. 8 (2016) 564–569.
[36] X.D. Wu, Z.X. Wang, L.Q. Chen, X.J. Huang, Solid State Ionics 170 (2004) 117–121.
[37] P. Zhou, W. Ren, G. Nie, et al., Angew. Chem. Int. Ed. 59 (2020) 16517–16526.
[38] P. Wang, S. Orimo, K. Tanabe, H. Fujii, J. Alloys Compd. 350 (2003) 218–221.
[39] K.E. Egili, E.F.E. Agammy, M.A. Zaibani, M. Jaremko, A.H. Emwas, Appl. Phys. A 127 (2021) 1–10.
[40] G.L. Richmond, Chem. Rev. 102 (2002) 2693–2724.
[41] B. Huang, Z. Xiong, P. Zhou, et al., J. Hazard. Mater. 424 (2022) 127641.
[42] Y. Qi, J. Li, Y. Zhang, et al., Appl. Catal. B: Environ. 286 (2021) 119910.
[43] G. Ye, P. Luo, Y. Zhao, et al., Chemosphere 253 (2020) 126767.
[44] G.V. Buxton, C.L. Greenstock, W.P. Helman, A.B. Ross, J. Phys. Chem. Ref. Data 17 (1988) 513–886.
[45] F.E. Scully, J. Hoigne, Chemosphere 16 (1987) 681–694.
[46] Y.M. Dong, G.L. Wang, P.P. Jiang, et al., Chin. Chem. Lett. 22 (2011) 209–212.
[47] Y. Ren, Q. Dong, J. Feng, et al., J. Colloid Interface Sci. 382 (2012) 90–96.
[48] W. Li, Z. Qiang, T. Zhang, F. Cao, Appl. Catal. B: Environ. 113 (2012) 290–295.
[49] S.M. Zhu, B.Z. Dong, Y.H. Yu, et al., Chem. Eng. J. 328 (2017) 527–535.
[50] A. Ranithri, Z. Sitian, W.Z. Yang, L.Y. Chen, LWT-Food. Sci. Technol. 158 (2022) 113162.
[51] M.C. DeRosa, R.J. Crutchley, Coord. Chem. Rev. 233 (2002) 351–371.
[52] J. Brame, M. Long, Q. Li, P. Alvarez, Water Res. 60 (2014) 259–266.
[53] L. Bu, N. Zhu, C. Li, et al., J. Hazard. Mater. 388 (2020) 121760.
[54] T. Zhang, C. Li, J. Ma, H. Tian, Z. Qiang, Appl. Catal. B: Environ. 82 (2008) 131–137.
[55] F. Qi, Z. Chen, B. Xu, et al., Appl. Catal. B: Environ. 84 (2008) 684–690.
[56] Guidelines for drinking-water quality: Fourth edition incorporating the first and second addenda, https://www.who.int/publications/i/item/9789240045064, June 18, 2022.